Available online at www.sciencedirect.com

ScienceDirect

Procedia Structural Integrity 13 (2018) 636–641

Structural Integrity Procedia

www.elsevier.com/locate/procedia

ECF22 - Loading and Environmental effects on Structural Integrity

Numerical and analytical model of long tubular bones with anisotropic distribution of elastic properties

Sergei Bosiakov[a,*], Kirill Yurkevich[a], Vadim V. Silberschmidt[b], Anna Ershova[a]

[a] *Belarusian State University, 4 Nezavisimosti Avenue, Minsk 220030, Belarus*
[b] *Loughborough University, Loughborough Leicestershire LE11 3TU, UK*

Abstract

Elastic parameters of a cortical bone tissue at the macrolevel can vary for various bones, as well as in different parts or anatomical quadrants, of the same bone. In this paper, an approach to finite-element modelling of the nonlinear anisotropic and isotropic distribution of elastic properties of tubular bones is proposed. Dependences of the Young's moduli, shear moduli and the Poisson's ratios on the spatial coordinates determining the position of the element in the bone model are used. They were obtained on the basis of experimental data on anisotropic elastic properties of tubular bone. A comparative finite-element analysis of the principal stresses and deformations caused by the action of own weight on the human femur was carried out for nonlinear anisotropic and isotropic distributions of elastic properties. Differences between the levels of maximum principal stresses and deformations for the three cases of elastic properties can reach approximately 10% and 30%, respectively.

Peer-review under responsibility of the ECF22 organizers.

Keywords: Long tubular bone; anisotropic elastic property; numerical and analytical model; principal stresses, deformation

1. Introduction

A bone tissue possesses anisotropy of mechanical properties both at microscale (osteons, havers channels, lamellae) and macroscale (entire bone) (Hoc et al. (2006); Rho et al. (1997); Roy et al. (1999)). In accordance with Goldstein (1987); Orías (2005); Li et al. (2013), values of the elastic parameters of a cortical bone tissue at the macroscale can vary between different bones, as well as in different parts (upper, middle and lower thirds) or anatomical quadrants (anterior, lateral, posterior and inner) of the same bone. These facts significantly affect the behavior of the bone tissue during routine human activities and traumatic effects on the entire bone (Currey (2012); Li et al. (2012)). At the same time, according to Hambli (2013), in most cases of finite-element modelling of bone tissue behavior under arbitrary loading, the bone tissue is simulated as an inhomogeneous and isotropic material. It usually employs empirical relations between the bone density and the modulus of elasticity to assign a single isotropic elastic modulus for each mesh element on the basis of computed tomography data.

* Corresponding author. Tel.: +375-29-722-4725 ; fax: +375-17-209-5249.
E-mail address: bosiakov@bsu.by

2452-3216
Peer-review under responsibility of the ECF22 organizers.
10.1016/j.prostr.2018.12.105

Bonnet et al. (2009); Gray et al. (2008); Koivumäki et al. (2012) and Yang et al. (2010) proposed approaches for the determination of anisotropic orientation of bone tissue, based on the dependence of cortical and trabecular structural morphology on mechanical behavior, as well as the use of anatomical directions corresponding to the shape of the bone. Models with an anisotropic distribution of elastic properties using the magnitudes of Hounsfield units of computed tomography based on micromechanical considerations were suggested by Hellmich et al. (2008); Schneider et al. (2009); Tabor and Rokita (2007); Trabelsi and Yosibash (2011) . A procedure for orienting of orthotropic properties in a proximal part of the finite-element model of femur based on directions of the principal stresses forced by the physiological load was presented by San Antonio et al. (2011). Hambli (2012); Hellmich et al. (2008); Juszczyk et al. (2011); Kaneko et al. (2003); Kotha and Guzelsu (2003) and Keaveny et al. (1999) proposed empirical relations between orthotropic mechanical constants and bone density.

In this study, an approach to modeling the elastic properties of a femur, based on the dependences of the elastic and shear moduli, and the Poisson's ratios on the coordinates for two-dimensional (2D) and one-dimensional (1D) cases are suggested; they are obtained on the basis of experimental data for various thirds and anatomical quadrants of the tubular bone.

2. Numerical and analytical modelling

2.1. 2D distribution of nonlinear anisotropic elastic poroperties

To describe the elastic properties of the femur bone, 2D regression functions were derived using the method of least squares on the basis of the elastic and shear moduli, and Poisson's ratios for twenty points located in the cortical bone tissue of diaphysis and approximately between trabecular and cortical bone in the different parts of femur. Twelve points A_k, L_k, P_k and M_k were located in corresponding anterior, lateral, posterior and medial anatomical quadrants of the femur cross section; every four points are in one of three different levels l_1, l_2 and l_3 of the diaphysis part of the thigh, $k = 1..3$. The eight points $A_0^{(n)}$, $L_0^{(n)}$, $P_0^{(n)}$ and $M_0^{(n)}$, $n = 1, 2$ were located in a trabecular bone tissue at levels m_1 and m_2 in the distal and proximal femur, respectively. The schematic location of the interpolation nodes at different levels of the femur is indicated in the Fig. 1.

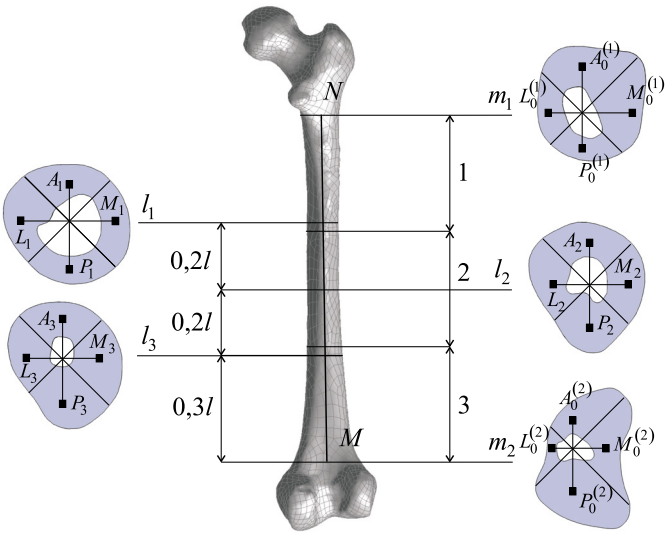

Fig. 1. Levels l_1, l_2 and l_3 of the femur diaphysis part with interpolation nodes A_k, L_k, P_k and M_k, $k = 1..3$; levels m_1 and m_2 are between the trabecular and cortical bone of femur with interpolation nodes $A_n^{(0)}$, $L_n^{(0)}$, $P_n^{(0)}$ and $M_n^{(0)}$, $n = 1, 2$; MN is the anatomical axis of the femur; l is the length of the femur part corresponding to cortical bone approximately; 1 is the upper third; 2 is the medium third; 3 is the lower third.

The trabecular bone tissue is modeled as a homogeneous isotropic material with the elastic modulus of 8.0 GPa and the Poisson's ratio of 0.3 according to Tanne and Sakuda (1991). Thus, in nodes $A_0^{(n)}$, $L_0^{(n)}$, $P_0^{(n)}$ and $M_0^{(n)}$, $n = 1, 2$

for trabecular bone tissue $E_1 = E_2 = E_3 = 8$ GPa, the Poisson's ratio $\nu_{12} = \nu_{13} = \nu_{23} = 0.3$ and the shear modulus $G_{12} = G_{13} = G_{23} = 3.08$ GPa are assigned for each anatomical quadrants. Values of the elastic constants in nodes A_k, L_k, P_k and M_k ($k = 1..3$) are given in Table 1 in accordance with Rho (1996). In Table 1 the indices 1, 2 and 3 correspond to the radial, circumferential and longitudinal directions; the longitudinal direction coincides with anatomical axis MN of the femur (see Fig. 1).

Table 1. Average elastic constants of cortical bone at different interpolation nodes in anterior, lateral, posterior and medial anatomical quadrants of femur cross section at levels l_1, l_2 and l_3 (indices 1, 2 and 3 for elastic constansts correspond to the radial, circumferential and longitudinal directions, respectively).

Interpolation node	E_1, GPa	E_2, GPa	E_3, GPa	G_{12}, GPa	G_{13}, GPa	G_{23}, GPa	ν_{12}	ν_{13}	ν_{23}
A_1	10.6	11.6	21.3	3.6	4.9	5.5	0.418	0.224	0.211
L_1	11.4	12.6	20.9	4.0	4.9	5.6	0.382	0.240	0.228
P_1	12.4	12.7	19.8	4.3	5.3	5.8	0.419	0.249	0.246
M_1	11.4	11.9	20.4	3.9	5.1	5.8	0.425	0.239	0.232
A_2	10.9	11.5	20.9	3.7	5.1	5.5	0.423	0.229	0.219
L_2	11.5	11.9	20.6	4.0	5.0	5.7	0.420	0.239	0.234
P_2	12.3	12.3	21.1	4.3	5.3	5.8	0.433	0.238	0.238
M_2	12.6	12.9	21.2	4.4	5.5	6.1	0.419	0.239	0.236
A_3	11.2	11.6	20.5	3.9	5.1	5.6	0.432	0.235	0.228
L_3	11.8	12.3	20.9	4.1	5.2	5.8	0.427	0.235	0.229
P_3	12.2	12.4	21.2	4.2	5.4	5.8	0.441	0.227	0.224
M_3	11.9	12.3	19.9	4.2	5.3	5.7	0.405	0.249	0.243

Regression functions for elastic constants were formulated on the assumption that in the radial direction the elastic properties of the femur bone within any cross section are unchanged. 2D dependences (A.1) – (A.9) of the elastic moduli, and Poisson's ratios on the longitudinal z and circumferential φ coordinates in the area between levels m_1 and m_2 of the femur are presented in Appendix A. The length of the femur part between levels m_1 and m_2 hereinafter is assumed to 0.31 m.

2.2. 1D distribution of anisotropic elastic poroperties

The elastic properties of the femur were modeled by using functions for the elastic and shear moduli, and Poisson's ratios only for the longitudinal coordinate z (varying along the anatomical axis of the femur MN indicated in Fig. 1). In this case, the cortical bone tissue is also a nonlinearly elastic orthotropic material. For regression functions, the averaged elasticity constants of bone are used in accordance with Rho (1996) at the level l_2 of the femur (see Fig. 1). The averaged values of the elastic moduli, shear moduli and Poisson's ratios at the level l_2 are given in the Table 2.

Table 2. Average elastic constants of cortical bone at interpolation nodes of the femur cross section at the level l_2.

E_1, GPa	E_2, GPa	E_3, GPa	G_{12}, GPa	G_{13}, GPa	G_{23}, GPa	ν_{12}	ν_{13}	ν_{23}
11.7	12.2	20.7	4.1	5.2	5.7	0.420	0.237	0.231

The trabecular bone at the levels m_1 and m_2 was assumed as an isotropic material, as well as in the 2D case (see Section 2.1). As a result of the polynomial interpolation, functions (A.10) for the elastic and shear moduli, and Poisson's ratios in dependence of the longitudinal coordinate z were derived. These functions are given in Appendix A.

2.3. Nonlinear isotropic elastic properties

The cortical bone tissue was modeled by a material with nonlinearly distributed isotropic properties along the anatomical axis of the femur, assuming non-changing elastic properties in the radial and circumferential directions in

any cross section of the bone. For the interpolation dependences of the elasticity modulus and the Poisson's ratio on the coordinate varying along the MN-axis (see the Fig. 1), the same elasticity moduli $E_1 = E_2 = E_3 = 14.9$ GPa and Poisson's ratios $\nu_{12} = \nu_{23} = \nu_{13} = 0.298$ of the cortical bone tissue were supposed at level l_2. The trabecular bone at levels m_1 and m_2 was also assumed as isotropic material, as in the two previous cases (see Sections 2.1 and 2.2).

Interpolation functions (A.11) for the elastic modulus and the Poisson's ratio vs z-coordinate, varying between the levels m_2 and m_1, are given in Appendix A.

3. Boundary conditions for static analysis

The load on the femur was applied along its biomechanical axis passing from the upper pole of the femoral head to the middle of the distance between the extreme lower sections of the condyles of the femur in accordance with Letter to the editor (2002) and Yoshioka et al. (1987). The region of application of the load was the third part of the upper segment of the head of the femur; the load magnitude was 800 N. The boundary conditions were defined in such a way that the femoral head (the acetabular contact region) and the lower sections of the condyles of the femur (the sites of contact with the condyles of the tibia) were rigidly embedded for modeling the self-weight action according to (Letter to the editor (2002)).

4. Discussion

The proposed approach to modelling the elastic properties of bone tissue makes it possible to assign their nonlinear anisotropic distribution along the anatomical axes and in cross section of the bone. The advantage of this approach is the use of statistical data on elastic and shear moduli, and Poisson's ratios for various parts and anatomical quadrants of bone, experimentally obtained for large amount of samples. Another advantage is the possibility of geometric transformation and modification of the bone model, e.g., for simulation of implantation, surgical operations, etc.

The calculated principal stresses and deformations caused by the action of own weight on the femur are significantly different for models with a nonlinear anisotropic and isotropic distributions of elastic properties. These differences can increase for more complex combined loading on the femur, e.g., for simultaneous action of self-weight and bending moments (for flexion-tension, aduction-abduction) or torque.

Acknowledgements

Authors acknowledge the Erasmus+ financial support, allowing visits of SB and KYu to Keele University, UK.

Appendix A. Spatial variation of elastic constants

$$\begin{aligned} E_1^{(1)}(\varphi, z) = {} & 0.00246775\varphi^3 - 0.0231933\varphi^2 + 0.0483053\varphi - 1.56228\varphi^3 z^3 + 3.707\varphi^2 z^3 - \\ & -156.394\varphi z^3 + 236.667 z^3 + 1.68187\varphi^3 z^2 - 19.6999\varphi^2 z^2 + 57.3801\varphi z^2 - 237.495 z^2 - \\ & -0.378222\varphi^3 z + 2.74996\varphi^2 z - 2.3469\varphi z + 51.7636 z + 8.0274, \end{aligned} \tag{A.1}$$

$$\begin{aligned} E_2^{(1)}(\varphi, z) = {} & 0.00335998\varphi^3 - 0.0324159\varphi^2 + 0.0710288\varphi - 10.936\varphi^3 z^3 + 108.328\varphi^2 z^3 - \\ & -248.909\varphi z^3 + 11.4181 z^3 + 5.68217\varphi^3 z^2 - 51.9547\varphi^2 z^2 + 102.118\varphi z^2 - 158.814 z^2 - \\ & -0.698451\varphi^3 z + 5.53273\varphi^2 z - 7.1894\varphi z + 49.6513 z + 8.04116, \end{aligned} \tag{A.2}$$

$$E_3^{(1)}(\varphi,z) = 8.92417\varphi^5z^5 - 141.19\varphi^4z^5 - 465.113\varphi^3z^5 + 8914.43\varphi^2z^5 - 16535.7\varphi z^5 - 47549z^5 + \\ +0.499524\varphi^5z^4 + 24.663\varphi^4z^4 + 21.1731\varphi^3z^4 - 1930.78\varphi^2z^4 + 4399.36\varphi z^4 + 14606z^4 - \\ -0.708928\varphi^5z^3 + 12.4988\varphi^4z^3 + 38.747\varphi^3z^3 - 804.607\varphi^2z^3 + 1530.39\varphi z^3 + 3946.05z^3 - \\ -0.337796\varphi^5z^2 - 1.43267\varphi^4z^2 + 7.74583\varphi^3z^2 + 167.768\varphi^2z^2 - 478.067\varphi z^2 - 2094z^2 + \\ +0.0707437\varphi^5z - 0.149099\varphi^4z - 2.26309\varphi^3z - 1.50093\varphi^2z + 25.5008\varphi z + 285.982z + 8, \tag{A.3}$$

$$G_{12}^{(1)}(\varphi,z) = 0.000948699\varphi^3 - 0.00846988\varphi^2 + 0.0157647\varphi - 3.12457\varphi^3z^3 + 39.9656\varphi^2z^3 - \\ -127.758\varphi z^3 + 117.295z^3 + 1.81964\varphi^3z^2 - 19.8852\varphi^2z^2 + 53.1055\varphi z^2 - 84.0534z^2 - \\ -0.26233\varphi^3z + 2.27077\varphi^2z - 3.91129\varphi z + 14.886z + 3.08892, \tag{A.4}$$

$$G_{13}^{(1)}(\varphi,z) = -8.4718\varphi^4z^4 + 942.252\varphi^3z^4 - 2766.15\varphi^2z^4 + 1382.9\varphi z^4 - 2534.05z^4 + \\ +52.2155\varphi^4z^3 - 570.234\varphi^3z^3 + 1636.59\varphi^2z^3 - 723.157\varphi z^3 + 1694.45z^3 - 9.74689\varphi^4z^2 + \\ +105.7\varphi^3z^2 - 296.994\varphi^2z^2 + 110.904\varphi z^2 - 438.142z^2 + 0.572878\varphi^4z - 6.30793\varphi^3z + \\ +18.0923\varphi^2z - 6.75303\varphi z + 49.7292z + 3.08, \tag{A.5}$$

$$G_{23}^{(1)}(\varphi,z) = -99.1473\varphi^4z^4 + 1106.29\varphi^3z^4 - 3579.05\varphi^2z^4 + 3406.66\varphi z^4 - 4963.65z^4 + \\ +62.957\varphi^4z^3 - 697.091\varphi^3z^3 + 2225.56\varphi^2z^3 - 2080.04\varphi z^3 + 3213.07z^3 - 12.0779\varphi^4z^2 + \\ +132.325\varphi^3z^2 - 413.578\varphi^2z^2 + 370.538\varphi z^2 - 747.317z^2 + 0.666983\varphi^4z - 7.21276\varphi^3z + \\ +21.726\varphi^2z - 17.2055\varphi z + 72.7723z + 3.08, \tag{A.6}$$

$$\nu_{12}^{(1)}(\varphi,z) = -6.06694\varphi^4z^4 + 81.7758\varphi^3z^4 - 355.482\varphi^2z^4 + 510.084\varphi z^4 - 246.139z^4 + \\ +4.03203\varphi^4z^3 - 53.1958\varphi^3z^3 + 225.005\varphi^2z^3 - 313.81\varphi z^3 + 162.615z^3 - 0.871705\varphi^4z^2 + \\ +11.1737\varphi^3z^2 - 45.4057\varphi^2z^2 + 60.3988\varphi z^2 - 38.7519z^2 + 0.0648672\varphi^4 - 0.807968\varphi^3z + \\ +3.13773\varphi^2z - 3.90792\varphi z + 3.81429z + 0.3, \tag{A.7}$$

$$\nu_{13}^{(1)}(\varphi,z) = 1.33336\varphi^4z^4 - 13.5821\varphi^3z^4 + 36.9715\varphi^2z^4 - 26.8389\varphi z^4 + 123.296z^4 - \\ -1.17659\varphi^4z^3 + 12.5201\varphi^3z^3 - 36.1896\varphi^2z^3 + 24.9636\varphi z^3 - 74.9134z^3 + \\ +0.332776\varphi^4z^2 - 3.6631\varphi^3z^2 + 11.1243\varphi^2z^2 - 7.82783\varphi z^2 + 16.6371z^2 - \\ -0.029697\varphi^4z + 0.335189\varphi^3z - 1.06546\varphi^2z + 0.828095\varphi z - 1.69293z + 0.3, \tag{A.8}$$

$$\nu_{23}^{(1)}(\varphi,z) = 0.251753\varphi^4z^4 + 0.410099\varphi^3z^4 - 21.7872\varphi^2z^4 + 58.2554\varphi z^4 + 141.462z^4 - \\ -0.524144\varphi^4z^3 + 4.14318\varphi^3z^3 - 1.06259\varphi^2z^3 - 26.8755\varphi z^3 - 84.3593z^3 + 0.210218\varphi^4z^2 - \\ -2.10589\varphi^3z^2 + 4.64254\varphi^2z^2 + 1.82261\varphi z^2 + 18.3066z^2 - 0.0218468\varphi^4z + 0.236185\varphi^3z - \\ -0.662882\varphi^2z + 0.259906\varphi z - 1.85513z + 0.3. \tag{A.9}$$

$$E_1^{(2)}(z) = -144.531z^2 + 46.25z + 8.0,\ E_2^{(2)}(z) = -164.063z^2 + 52.5z + 8.0, \\ E_3^{(2)}(z) = -496.094z^2 + 158.75z + 8.0,\ G_{12}^{(2)}(z) = -48.4375z^2 + 15.5z + 2.86, \\ G_{13}^{(2)}(z) = -90.2344z^2 + 28.875z + 2.86,\ G_{23}^{(2)}(z) = -110.938z^2 + 35.5z + 2.86, \\ \nu_{12}^{(2)}(z) = -4.6875z^2 + 1.5z + 0.3,\ \nu_{13}^{(2)}(z) = 2.46094z^2 - 0.7875z + 0.3, \\ \nu_{23}^{(2)}(z) = 2.69531z^2 - 0.8625z + 0.3. \tag{A.10}$$

$$E^{(3)}(z) = -269.531z^2 + 86.25z + 8,\ \nu^{(3)}(z) = 0.3 - 0.025z + 0.078125z^2. \tag{A.11}$$

References

Bonnet, A.S., Postaire, M., Lipinski, P., 2009. Biomechanical study of mandible bone supporting a four-implant retained bridge finite element analysis of the influence of bone anisotropy and foodstuff position. Medical Engineering and Physics 31, 806-815.

Currey, J.D., 2012. The structure and mechanics of bone. Journal of Material Science 47, 41–54.

Goldstein, S., 1987. The mechanical properties of trabecular bone: dependence on anatomic location and function. Journal of Biomechanics 20, 1055–1061.

Gray, H.A., Taddei F., Zavatsky, A.B., Cristofolini, L., Gill, H.S., 2008. Experimental validation of a finite element model of a human cadaveric tibia. Journal of Biomechanical Engineering 130, 031016.

Hambli, R., 2011. Apparent damage accumulation in cancellous bone using neural networks. Journal of the Mechanical Behavior of Biomedical Materials 4, 868-878.

Hambli, R., 2013. A quasi-brittle continuum damage finite element model of the human proximal femur based on element deletion. // Medical and Biological Engineering and Computing 51, 219–231.

Hellmich, C., Kober, C., Erdmann, B., 2008. Micromechanics-based conversion of CT data into anisotropic elasticity tensors, applied to FE simulations of a mandible. Annals of Biomedical Engineering 36, 108-122.

Hoc, T., Henry, L., Verdier, M., Aubry, D., Sedel, L., Meunier, A., 2006. Effect of microstructure on the mechanical properties of haversian cortical bone. Bone 38, 466–474.

Juszczyk, M.M., Cristofolini, L., Viceconti, M., 2011. The human proximal femur behaves linearly elastic up to failure under physiological loading conditions. Journal of Biomechanics 44, 2259-2266.

Kaneko, T.S., Pejcic, M.R., Tehranzadeh, J., Keyak, J.H., 2003. Relationships between material properties and CT scan data of cortical bone with and without metastatic lesions.Medical Engineering and Physics 25, 445-454.

Keaveny, T.M., Wachtel E.F., Kopperdahl D.L., 1999. Mechanical behavior of human trabecular bone after overloading. Journal of Orthopaedic Research 17, 346-353.

Koivumäki, J.E., Thevenot, J., Pulkkinen, P., Kuhn, V., Link, T.M., Eckstein, F., Jämsä T., 2012. CT-based finite element models can be used to estimate experimentally measured failure loads in the proximal femur. Bone 50, 824-829.

Kotha, S.P., Guzelsu, N., 2003. Tensile damage and its effects on cortical bone. Journal of Biomechanics 36, 1683-1689.

Letter to the editor, 2002. ISB recommendation on definitions of joint coordinate system of various joints for the reporting of human joint motion part I: ankle, hip, and spine. Journal of Biomechanics 35, 543548.

Li, S., Abdel-Wahab, A.A, Silberschmidt, V.V., 2012. Analysis of fracture processes in cortical bone tissue. Engineering Fracture Mechanics 110, 448–458.

Li, S., Demirci, E., Silberschmidt, V.V. 2013. Variability and anisotropy of mechanical behaviour of cortical bone in tension and compression. Journal of Mechanical Behavior of Biomedical Materials 21, 109–120.

Orías, A.A.E., 2005. The relationship between the mechanical anisotropy of human cortical bone tissue and its microstructure. Dissertation. Notre Dame, Indiana, USA, pp. 142.

Rho, J.Y., 1996. An ultrasonic method for measuring the elastic properties of human tibial cortical and cancellous bone. Ultrasonics 34, 777–783.

Rho, J. Tsui, T.Y., Pharr, G.M., 1997. Elastic properties of human cortical and trabecular lamellar bone measured by nanoindentation. Biomaterials 18, 1325–1330.

Roy, M.E., Rho, J., Tsui, T.Y., Evans, N.D., Pharr, G.M., 1999. Mechanical and morphological variation of the human lumbar vertebral cortical and trabecular bone. Journal of Biomedical Materials Research 44, 191–197.

San Antonio, T., Ciaccia, M., Muller-Karger, C., Casanova, E., 2011. Orientation of orthotropic material properties in a femur FE model: a method based on the principal stresses directions. Medical Engineering and Physics 34, 914-919.

Schneider, R., Faust, G., Hindenlang, U., Helwig, P., 2009. Inhomogeneous, orthotropic material model for the cortical structure of long bones modeled on the basis of clinical CT or density data. Computer Methods in Applied Mechanics and Engineering 198, 2167-2174.

Tabor, Z., Rokita, E., 2007. Quantifying anisotropy of trabecular bone from gray-level images. Bone 40, 966-972.

Tanne, K., Sakuda M., 1991. Biomechanical and clinical changes of the craniofacial complex from orthopedic maxillary protraction. Angle Orthodontist 61, 145–152.

Trabelsi, N., Yosibash, Z., 2011. Patient-specific finite-element analyses of the proximal femur with orthotropic material properties validated by experiments. Journal of Biomechanical Engineering 133, 061001.

Yang, H., Ma, X., Guo, T., 2010. Some factors that affect the comparison between isotropic and orthotropic inhomogeneous finite element material models of femur. Medical Engineering and Physics 32, 553-560.

Yoshioka Y., Siu D., Cooke D.V., Chir B., 1987. The anatomy and functional axes of the femur. Journal of Bone and Joint Surgery 69-A, 873–880.